chemosensors

MDPI

Article

Electrochemical Sensing Platform Based on Renewable Carbon Modified with Antimony Nanoparticles for Methylparaben Detection in Personal Care Products

Gabriela Contesa Gomes, Martin Kássio Leme da Silva, Francisco Contini Barreto and Ivana Cesarino *

Department of Bioprocess and Biotechnology, School of Agriculture, São Paulo State University, Botucatu 18610-034, SP, Brazil

* Correspondence: ivana.cesarino@unesp.br; Tel.: +55-(14)-3880-7404

Abstract: This paper describes for the first time the surface modification of glassy carbon (GC) electrodes with bamboo-based renewable carbon (RC) and antimony nanoparticles (SbNPs) for the determination of methylparaben (MePa) in personal care products (PCPs). The synthesized RC-SbNP material was successfully characterized by scanning electron microcopy, energy-dispersive X-ray spectroscopy and cyclic voltammetry. The proposed sensor was applied in the detection of MePa using the optimized parameters by differential pulse voltammetry (DPV). The analytical range for detection of MePa was 0.2 to 9.0 μmol L^{-1}, with limits of detection and quantification of 0.05 μmol L^{-1} and 0.16 μmol L^{-1}, respectively. The determination of MePa in real PCP samples was performed using the proposed GC/RC-SbNP sensor by DPV and UV-vis spectrophotometry as comparative methodology. The use of RC-SbNP material for the development of electrochemical sensors brings a fresh approach to low-cost devices for MePa analysis.

Keywords: renewable carbon; antimony nanoparticles; methylparaben; personal care products; electrochemical sensors

check for updates

Citation: Gomes, G.C.; da Silva, M.K.L.; Barreto, F.C.; Cesarino, I. Electrochemical Sensing Platform Based on Renewable Carbon Modified with Antimony Nanoparticles for Methylparaben Detection in Personal Care Products. *Chemosensors* **2023**, *11*, 141. https://doi.org/10.3390/chemosensors11020141

Academic Editor: Jose V. Ros-Lis

Received: 24 December 2022
Revised: 7 February 2023
Accepted: 13 February 2023
Published: 15 February 2023

Copyright: © 2023 by the authors. Licensee MDPI, Basel, Switzerland. This article is an open access article distributed under the terms and conditions of the Creative Commons Attribution (CC BY) license (https://creativecommons.org/licenses/by/4.0/).

1. Introduction

Due to globalization, there has been an increase in the use of pharmaceuticals and personal care products (PCPs) in the last decade. PCPs are a class of emerging environmental contaminants considered hazardous molecules that may interfere with aquatic environments, leading to physiological effects through excessive exposure to humans and animals [1–3].

Methylparaben (MePa), as well as parabens in general, is a well-known antibacterial and antifungal preservative used in foods, pharmaceuticals, and PCPs due to such characteristics as high hydrophilicity and water solubility and to prolong storage time of the products. In addition, MePa is the most common paraben used in these industries and is considered safe to humans [4–7]. However, recent studies revealed that such compounds are considered hazardous due to their ability to competitively bind to estrogen receptors, leading to endocrine problems in the immune system and nervous systems and the production/degradation of endogenous steroids [8–10]. Parabens in general can also be viewed as endocrine-disrupting compounds (EDCs) [11]. The presence of such contaminants in different products has been associated with ovary and womb cancer in women. In addition, some works reported the presence of MePa in blood and urine samples of children [8,12]. In some countries, its use has already been restricted and usage limits defined. In an environmental context, due to its wide use, methylparaben is one of the most detected parabens in effluent [13], being present in the aquatic ecosystem [14]. Despite this, its potential ecotoxicity effects are not elucidated, still requiring studies [15]. The European Union (EU) has stablished a 0.8% *w*/*w* maximum concentration for total of parabens in commercial products [16].

In the last decade, several analytical methodologies have been developed to detect MePa [17,18]. Chromatographic methods coupled with mass spectrometry are currently the most used technique for detecting such contaminants [19–21]. However, such techniques can require solid phase extraction (SPE) [22], extraction, and cleanup based on Quick Easy Cheap Effective Rugged Safe (QuEChERS) methods [23], high-quality solvents (chromatography grade), and highly trained personnel. In order to overcome such restrictions, electrochemical sensors have been extensively used to detect endocrine compounds (ECs) and EDCs [24]. Advantageous characteristics of electrochemical sensors, such as highly sensitive and rapid analysis and low-cost equipment, have gained attention in the development of analytical protocols for the detection of such chemicals [25–30].

Electrochemical sensors based on carbon-based materials are at the forefront of sensing research due to the intrinsic properties of carbon of high electrical conductivity, mechanical strength, chemical stability, and surface-to-volume ratio [31]. In addition to the use of 0D, 1D, 2D, and 3D carbon materials in sensors, renewable carbon, also known as biochar, has recently become an interesting option for manufacturing electrochemical sensor platforms [32–34].

Renewable carbon (RC) is a carbon-based material originating from the slow pyrolysis of biomass and has gained prominence due to its highly functionalized and porous surface characteristics, which can lead to interesting applications of inorganic molecules (heavy metal ions) [35], organic molecules (e.g., ECs and EDCs) [36,37], and biosensing assays [38] (e.g., SARS-CoV-2) [39]. The modification and decoration of RC with different metal/metal oxides micro/nanoparticles have been investigated in order to maximize the electrical current response for electroactive molecules due to the synergistic, catalytic effect, thus facilitating electron transfer [40–42]. Antimony nanoparticles (SbNPs) have been applied for modification of carbon-based materials due to favorably negative overvoltage of hydrogen evolution, wide operational potential window, convenient operation in acidic solutions of pH 2 or lower, and a very small Sb stripping signal [43–45].

In this work, we report the modification of glassy carbon electrodes using the RC material modified with Sb nanoparticles. The morphological, structural, and electrochemical characterization of an RC-SbNP nanocomposite was properly evaluated. The proposed sensor was applied in the detection of MePa in buffer solutions and then in real PCP samples using differential pulse voltammetry (DPV). A comparative methodology by UV-vis spectrophotometry was used for verifying the reliability of the new electrochemical sensor.

2. Materials and Methods

2.1. Instrumentation and Methods

The voltammetric experiments were carried out using an electrochemical system model—Autolab PGSTAT128N Metrohm (Eco Chemie, Utrecht, The Netherlands)—equipped with NOVA 2.1 software. A conventional glass electrochemical cell with three electrodes was used to carry out the experiments: a glassy carbon electrode modified (2 mm $\pm$ 0.1 mm) with RC-SbNPs as the working electrode, the Ag/AgCl/KCl (3.0 mol L^{-1}) electrode as the electrode reference plate, and a platinum plate as an auxiliary electrode.

The electrochemical characterization of the GC/RC-SbNP electrode was carried out using cyclic voltammetry from -1.0 to + 0.6 V vs. Ag/AgCl/KCl (3.0 mol L^{-1}) in a 0.5 mol L^{-1} HCl solution with a scan rate of 50 mV s^{-1}.

The morphology of the RC-SbNP material was characterized by scanning electron microcopy (SEM, JEOL, model JSM-7500F) and energy-dispersive X-ray spectroscopy (EDS, ultradry, Thermo Scientific) at the Institute of Chemistry (IQ) at UNESP, Araraquara, Brazil.

2.2. Reagents and Solutions

All reagents used in this work were analytical and used without prior purification. Bamboo-based renewable carbon (RC) obtained through pyrolysis of bamboo biomass was kindly provided by Mohini Sain of the University of Toronto. The $SbCl_3$ salt, methylparaben

standard, was purchased from Sigma-Aldrich. All solutions were prepared using purified water in a PureLab Option-Q ELGA-Veolia system (resistivity $\geq$ 18 MΩ cm^{-1}).

2.3. Synthesis of RC-Antimony Nanoparticles

The synthesis of the RC-SbNPs was carried out by a chemical reduction process reported in previous works [44,46]. Briefly, 40 mg of RC was added to a beaker with 30 mL of ethanol, and the mixture was homogenized by using an ultrasonic cell disruptor (QSonica) for 15 min. Then, 16 mg of a surfactant, sodium dodecyl sulfate (SDS), was added and a 15 min ultrasonic bath carried out. For the chemical reduction process, 26 mg of sodium borohydride ($NaBH_4$) were added, and the solution was sonicated for an additional hour. Finally, the Sb nanoparticles were incorporated into the carbon material by adding a 1 mg/mL $SbCl_3$ solution under vigorous stirring (1 drop per second). The obtained RC-SbNP material was centrifuged and cleaned several times with ethanol, and dried at 60 °C (overnight).

Finally, a dispersion of RC and RC-SbNPs, 1 mg/mL of each material, was prepared in ultrapure water for the electrode's modification. The materials were sonicated in an ultrasonic cell disruptor (QSonica) for 1 cycle of 10 min prior to use.

2.4. Electrode Preparation

Cleaning of the glassy carbon (GC) electrodes was done by polishing followed by an ultrasound bath. Polishing was carried out until a mirrored surface was obtained in a polishing machine with sandpaper made of silicon carbide and an aqueous suspension of 0.5 µm alumina. Soon afterward, the electrodes were put in an ultrasound bath in ethanol for 5 min and then in ultrapure water for another 5 min. After the polished GC electrodes had been cleaned and dried at room temperature, 10 µL of the suspension to be studied (RC or RC-SbNPs) was added. The suspension was dried at room temperature and the electrodes taken to the electrochemical cell to perform voltammetry studies. Scheme 1 summarizes the synthesis process of RC-SbNPs, the modification of GC electrodes with the nanocomposite and the electrochemical system used in this paper.

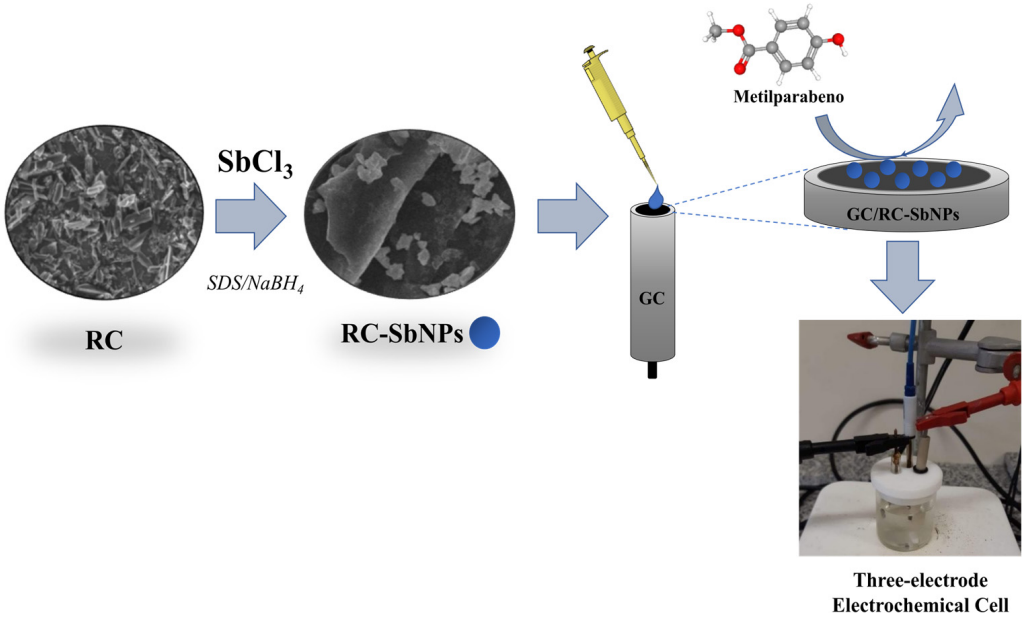

Scheme 1. Summary of the GC/RC-SbNP sensor fabrication and electrochemical setup.

2.5. Analysis of Methylparaben in PCPs

Five different samples of PCPs were purchased at a local supermarket in Botucatu, São Paulo, Brazil. Hand sanitizer (ethyl alcohol 70°), mouthwash, deodorant, emollient for cuticles, and a moisturizer cream were chosen for analysis according to the presence of

methylparaben as a constituent in the formulation, as reported on their labels. All samples were diluted 1:10 in ethanol, in order to perform a liquid–liquid/liquid–solid extraction of MePa. In addition, after the dilution in ethanol, the samples of deodorant, emollient for cuticles, and moisturizer cream were diluted in 100 mL of PBS (pH 7.0) and centrifuged in order to obtain a solid/liquid phase separation and thus facilitate the electrochemical and spectrophotometric experiments. After proper dilution, an aliquot of 0.25 mL was added to a 20 mL electrochemical cell with 0.1 mol L^{-1} PBS (pH 7.0).

The quantitative analysis of MePa was carried out by the standard addition method, in which known concentrations of the standard were added during the analysis. This is a quantitative analysis method, which is often used when the sample of interest has multiple components that result in matrix effects, where the additional components may either reduce or enhance the analyte absorbance signal [47].

For validation of the electroanalytical methodology, the samples were also analyzed in a UV-visible spectrophotometer (mono-beam) model UV-M51 by BEL Engineering®, Monza (Milano), Italia. A wavelength scan was carried out from 220 to 350 nm, with a step of 1 nm per point of reading. The samples were also enriched with known amounts of MePa reference standard. The obtained results for the UV-vis and DPV techniques were used to compare the amounts of MePa.

3. Results

3.1. Morphological and Spectroscopic Characterization of the RC-SbNP Composite

Surface morphology characterization was carried out by FEG-SEM analyses. As shown in Figure 1A, the RC materials display a very heterogeneous structure in arrangement and size, which is important, as it provides a high contact surface and a better conductivity, both good characteristics for use in electrochemical processes. Figure 1B,C show the RC-SbNP nanomaterial at different magnitudes, and the inclusion of Sb nanoparticles with mean size of 50 nm (Figure 1D). Figure 1E shows the EDS spectra obtained from the RC-SbNP nanocomposite, confirming the composition of the material with carbon (0.255 eV), oxygen (0.522 eV) and antimony (3.60 eV).

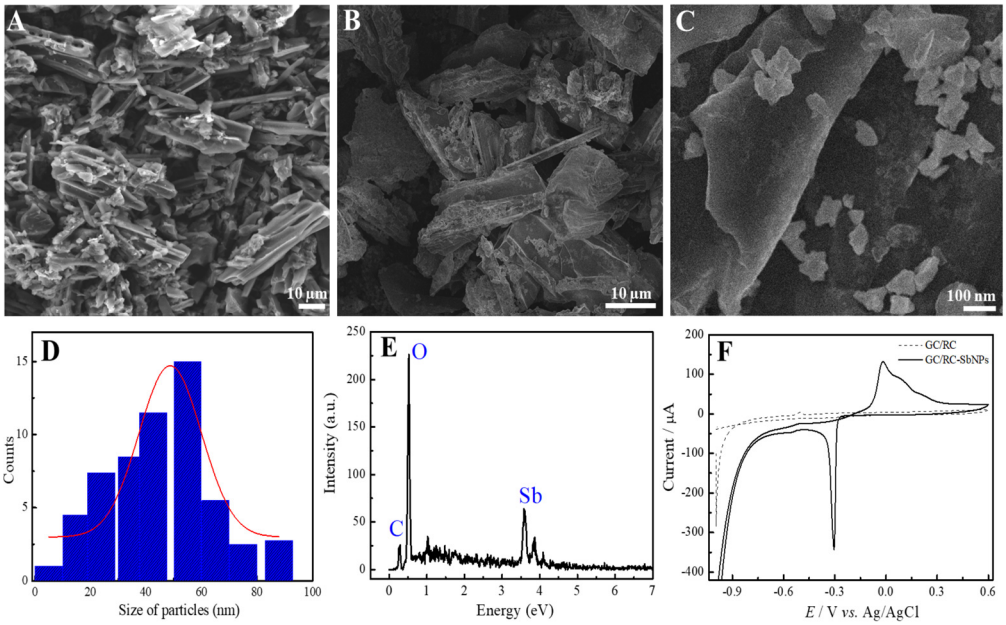

Figure 1. Morphological characterization by FEG-SEM of (**A**) RC, (**B**) RC-SbNPs and (**C**) SbNPs at higher magnitude. (**D**) Size distribution of Sb nanoparticles. (**E**) EDS spectra of RC-SbNPs. (**F**) Cyclic voltammetry of the GC/RC-SbNP (dashed line) and GC/RC-SbNP (solid line) electrodes in 0.5 mol L^{-1} HCL, with scan rate of 50 mV s^{-1}.

Electrochemically, the characterization of the composite containing antimony was performed by cyclic voltammetry experiments with a scan rate of 50 mV s^{-1} in a 0.5 mol L^{-1} HCl solution. The comparison was between the GC electrode modified only with the RC and the GC electrode modified with RC-SbNPs. In Figure 1F, it is possible to observe that in the GC/RC electrode (dashed line) no electrochemical processes occurred. On the contrary, when the GC/RC-SbNPs was used (solid line), it was possible to see an electrochemical process referring to the antimony nanoparticles. The oxidation peak shown in GC/RC-SbNP electrode voltammetry at 19 mV (solid line) is associated with deoxidation of Sb^0 to Sb^{+3}. In the reverse scan, it is possible to observe a reduction process of Sb at −305 mV. Therefore, we can conclude that the electrochemical processes present in the voltammogram correspond to the presence of Sb on the electrode surface, which proves that the nanoparticles were well incorporated into the GC/RC [36,44,46,48,49].

3.2. Electrochemical Characterization of the GC/RC-SbNP Electrode

Electrochemical characterization of the construction steps of the GC/RC-SbNP sensor was carried out using CV and EIS experiments. Figure S1A shows the voltammetric response of the unmodified GC electrode (dashed line), GC/RC (solid red line) and GC/RC-SbNPs (solid blue line). It was possible to observe well-defined oxidation and reduction processes for the $[Fe(CN)_6]^{4-/3-}$ redox probe. It is worth noting that the anodic (I_{pa}) and cathodic (I_{pc}) currents increased with the modification of electrodes with RC and RC-SbNPs. In addition, the reversibility of the redox process was improved, as shown in Table S1. The GC electrode presented a peak separation (ΔE_p) of 493 mV, followed by the GC/RC with a ΔE_p of 385.10 mV, and the GC/RC-SbNPs with 406.50 mV. In Figure S2B, as anticipated, the GC electrode presented a higher resistance to charge transfer (R_{ct}) in the order of 3.73 kΩ. After the electrode modification with RC and RC-SbNP nanomaterials, the (R_{ct}) decreased to 2.81 and 2.70 kΩ, respectively. The EIS results were fitted in a Randles equivalent circuit consisting of electrolyte or cell resistance (R_s), in series with a parallel combination of a constant phase element (CPE), which was used to represent the nonideal capacitance C, and charge-transfer resistance (R_{ct}) in series with Warburg impedance (W). The results for EIS experiments are summarized in Table S2 (Supplementary Materials). These results indicate that there is an improvement in electron kinetics in the electrode/electrolyte surface, thus improving the response in both CV and EIS experiments.

3.3. Methylparaben Oxidation Process

The electrochemical behavior of MePa on the GC/RC-SbNP electrode was performed by cyclic voltammetry (CV) with scan rate of 50 mV s^{-1} in phosphate buffer solution (PBS) 0.1 mol L^{-1} pH 7.0, added to 100.0 µmol L^{-1} of methylparaben. The results shown in Figure 2A revealed no electrochemical process in the absence of the analyte (dashed line). However, in the presence of 100 µmol L^{-1} of MePa (solid line), an irreversible oxidation peak could be observed at E_{pa} = +0.878 V vs. Ag/AgCl/KCl (3.0 mol L^{-1}). This oxidation process is similar to the findings reported by Piovesan et al. [27]: a defined peak close to 0.86 V. The inset in Figure 2A shows the respective redox reaction involved with this molecule. The oxidation of phenolic compounds can usually occur by a single-electron and proton transfer. This mechanism was further investigated by Gil et al. [50], reporting different parabens oxidize in the potential range. Slight differences in oxidation peak may be observed due to the length of the carbon chain.

Figure 2B shows the effect of the variation in scan rate on the oxidation process of MePa between 10 mV s^{-1} and 75 mV s^{-1}. The plot log I_{pa} vs log scan rate (mV s^{-1}) revealed a linear relationship with R^2 of 0.9974 and slope of 0.5833. According to the literature [41], a log–log plot slope of (or close to) 0.5 indicates a diffusion-controlled reaction rate [27]. Differential pulse voltammograms were recorded in a 0.1 mol L^{-1} PBS pH 7.0 solution added to 10.0 µmol L^{-1} of MePa in order to compare the voltammetric response of the analyte at the bare and modified electrodes. Figure 2C shows the results obtained for the GC (dash line), GC/RC (curve a) and GC/RC-SbNP (curve b) electrodes. It is possible

to observe once again the influence of antimony nanoparticles on RC for the detection of methylparaben, since the value of the anodic peak current is higher than the one that does not present the nanoparticles, showing efficiency in its use for detection. The anodic peak current increased by a factor of 4.4 and 6.8 for the GC/RC and RC/RC-SbNP electrodes, respectively, when compared to the unmodified one. These findings can be attributed to the adsorptive characteristics of RC, reported in literature to have a highly porous functionalized structure and high surface area [32,51]. Therefore, phenolic compounds such as MePa can be easily adsorbed on the carbon surface through hydrogen binding, physical adsorption, or p–p stacking of electrons of the carbon chain [37]. The addition of Sb nanoparticles has been reported to create a synergetic effect with carbon nanomaterials (e.g., biochar, carbon nanotubes, graphene) [43,52,53].

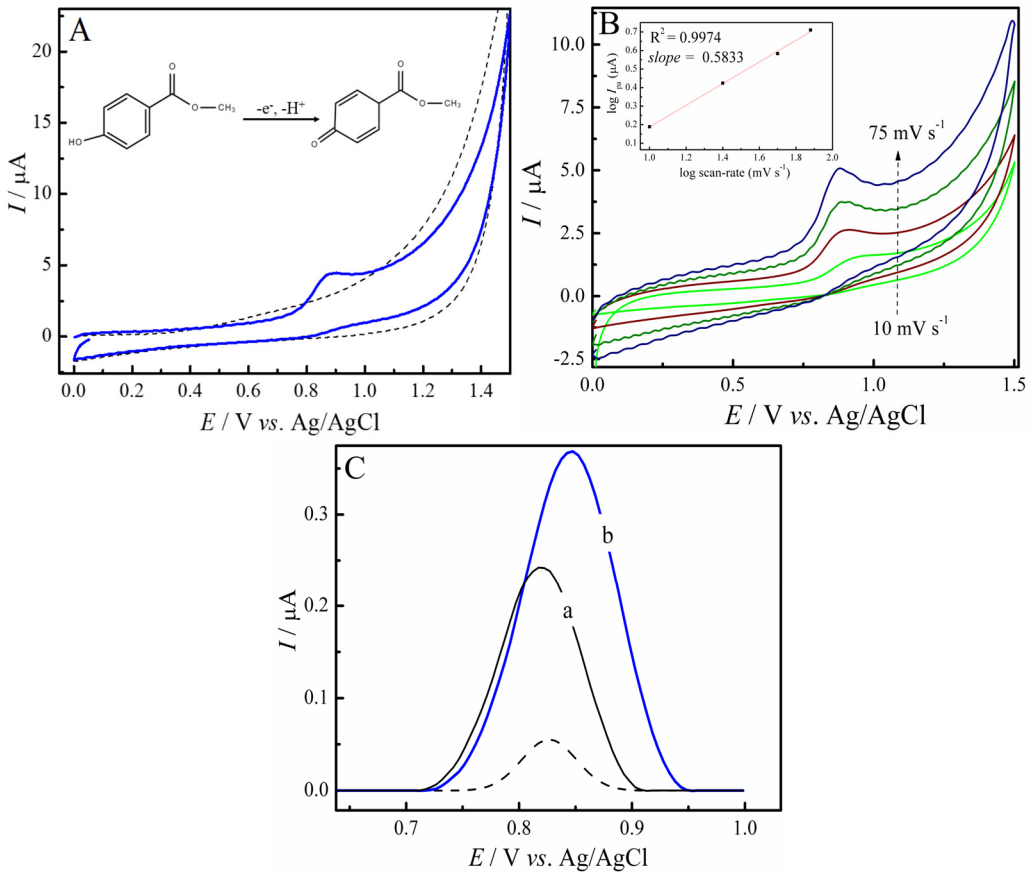

Figure 2. (**A**) Cyclic voltammetry at GC/RC-SbNP electrode in 0.1 mol L^{-1} PBS (pH 7.0) solution in the absence (dashed line) and presence (solid line) of 100 µmol L^{-1} MePa. (**B**) Cyclic voltammetry at GC/RC-SbNPs in 0.1 mol L^{-1} PBS (pH 7.0) in the presence of 100 µmol L^{-1} of dopamine, evidencing a linear increase for anodic peak in the function of the increase of scan rate. (**C**) Differential pulse voltammograms in 0.1 mol L^{-1} PBS pH 7.0 solution added to 10.0 µmol L^{-1} of MePa for GC electrode (dash line), GC/RC electrode (a) and GC/RC-SbNP electrode (b).

3.4. Influence of pH on the Oxidation Process of Methylparaben Using the GC/RC-SbNP Electrode

The optimization study of the electrolyte's pH regarding the redox process in 100.0 µmol L^{-1} of MePa was conducted by DPV experiments at the GC/RC-SbNP electrode. The pH of 0.1 mol L^{-1} PBS ranged from 5.0 to 10.0, the best response that could be obtained with the analyte. Figure 3A shows the comparative DPV experiments at different pH for 10.0 µmol L^{-1} of MePa, showing the change in the oxidation processes of this phenolic compound. In Figure 3B, it is possible to observe a dependent relation between the anodic peak current (I_{pa}) and the pH variation. The graph also shows that the peak anodic current has a maximum value of exactly pH 7.0, so this value was chosen and used

in the following analysis. For the oxidation potential (E_{pa}), we can notice the change in the potential, where MePa moves towards more negative values as the pH increases, which is related to the reduction in ionic concentration of hydrogen, pointing to the deprotonation process that occurs during oxidation. The plot E_{pa} vs. pH presents a linear regression (Figure 3B), with a slope of −55.4 mV, which indicates that the MePa oxidation involves the participation of the same number of protons and electrons. This is a process with a previously reported mechanism for the oxidation of methylparaben that involves two protons and two electrons [54,55]. The inflection point between pH 8.0 and 9.0 corresponds to the pk_a of analyte, similar to the value of 8.17 reported in the literature [56]. In addition, the results indicated that MePa has a higher anodic current response when 0.1 mol L^{-1} PBS solution at pH 7.0 is used as a supporting electrolyte. Therefore, this solution was used for the subsequent analyses.

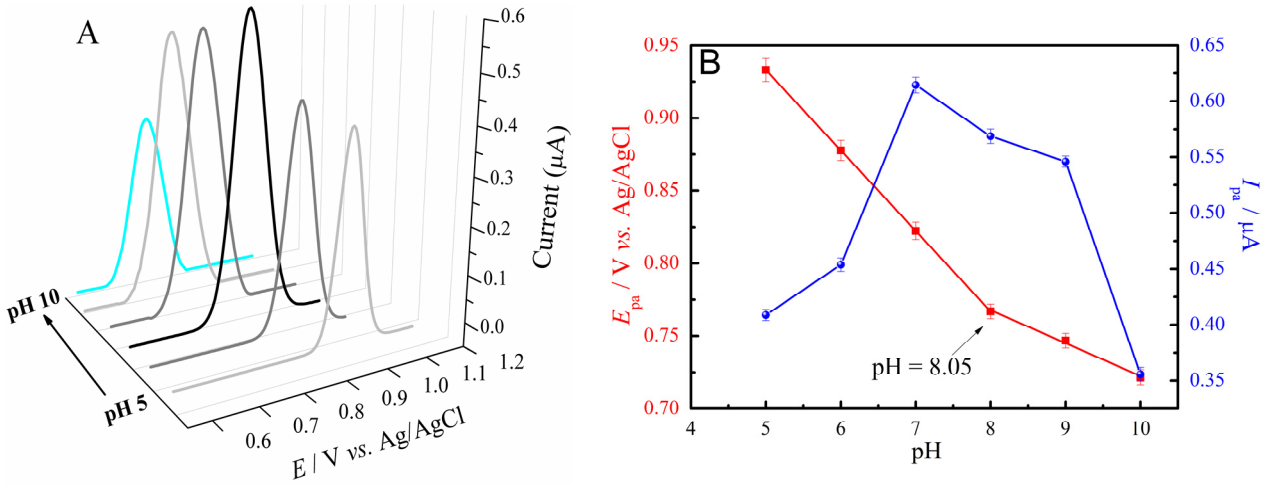

Figure 3. (**A**) DPV voltammograms using the GC/RC-SbNP electrode in the presence of 10.0 μmol L^{-1} in a 0.1 mol L^{-1} PBS solution at different pH, from 5.0 to 10. (**B**) Effect in I_{pa} (■) and E_{pa} (●) as a function of pH of the buffer solution.

3.5. Optimization of the Electrode Composition in the Voltammetric Response of Methylparaben Using the GC/RC-SbNP Electrode

Another important parameter optimized was the influence of RC-SbNP film concentration on the electrode, which was obtained performing a DPV with five different electrodes varying composite concentration from 0.5 to 2.0 mg/mL at an amplitude of 100 mV and a scan rate of 10 mV s^{-1} in a 0.1 mol L^{-1} PBS solution pH 7.0 added to 10.0 μmol L^{-1} MePa. As shown in Figure S2, we can observe that the concentration film that presented the highest anodic peak current (I_{pa}) was 1.0 mg mL^{-1} when used for the modification of the electrode. Therefore, for all the following experiments and analysis of MePa, this concentration was applied.

3.6. Calibration Curve and Detection and Quantification Limits

Figure 4A presents the DPV experiments using the proposed GC/RC-SbNP electrode, following all the optimized conditions described during the work. The voltammogram presented a linear region from 0.2 to 9.0 μmol L^{-1} with additions of MePa, according to the equation presented (Figure 4B) with a correlation coefficient of 0.990 (n = 9). According to the IUPAC recommendations, the limit of detection (LOD) was found to be 0.05 μmol L^{-1}, which was determined using the 3σ/slope, where σ is the standard deviation of 10 voltammograms from the blank. The limit of quantification (LOQ) obtained was 0.16 μmol L^{-1} determined by 10σ/slope, also as recommended by the IUPAC.

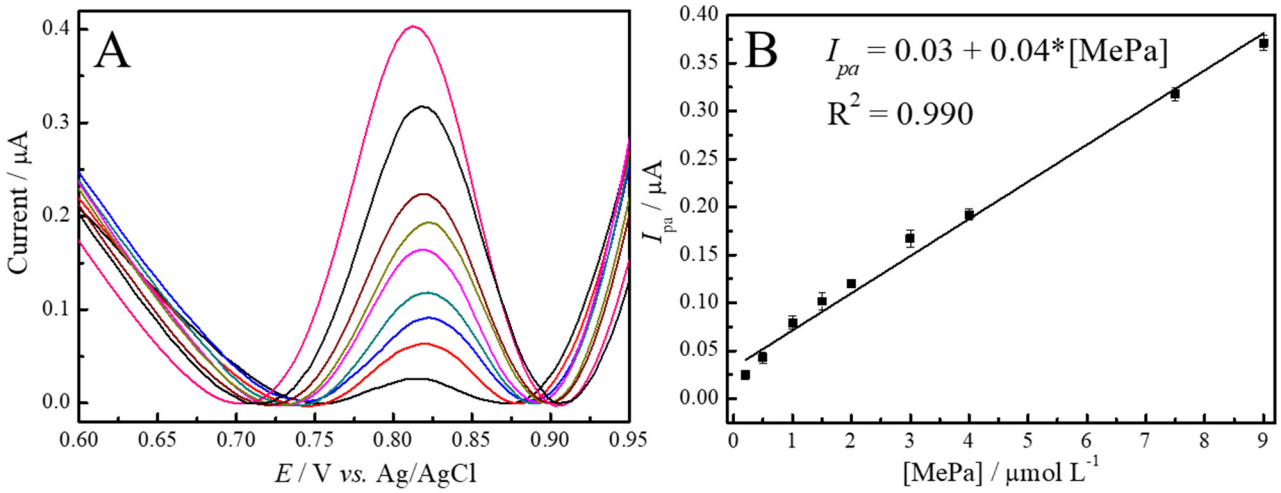

Figure 4. (**A**) Differential pulse voltammograms using GC/RC-SbNPs in 0.1 mol L^{-1} PBS pH 7.0 solution at different concentrations of MePa. (**B**) Linear relation between peak anodic currents and the MePa concentrations.

Table 1 shows the comparison of different electrodes reported in the literature and their respective analytical parameters for MePa determination. In comparison to previous reports, the LOD reported herein in this manuscript offered a good working range of concentration for the detection of MePa in PCP samples. There are some noteworthy works in the literature regarding the electrochemical detection of methylparaben and other parabens. Piovesan et al. [27] reported a modified electrode based on reduced graphene oxide (rGO) and gold nanoparticles (AuNP) dispersed in chitosan (CS) for the voltammetric determination of methylparaben (MePa). The authors reported a linear range of voltammetric detection from 0.03 to 1.30 µmol L^{-1} (R^2 = 0.990), with a LOD of 13.77 µmol L^{-1} and a LOQ of 41.73 µmol L^{-1}. The AuNP-rGO-CS/GCE was also applied in the detection of MePa in PCPs with recovery ranging from 84.3% to 133.5%. The use of carbon-based materials for electrode modification, such as rGO [57] and multiwalled carbon nanotubes (MWCNTs) [58], showed great sensitivity toward MePa detection. In particular, the work reported by Baytak et al. [59], a GCE modified with carbon nanofibers (CNFs) and nickel–cobalt–palladium nanoparticles showed an LOD of 0.0012 µmol L^{-1}, the lowest reported to our knowledge. Although some papers discussed in this manuscript showed lower LODs, the GC/RC-SbNP sensor displayed a linear range in concentrations suitable for detecting MePa in PCP samples. Therefore, the next section covers the application of the proposed sensor in real samples.

3.7. Determination of MePa in PCPs

The GC/RC-SbNP electrode was applied in the determination of MePa in real PCPs samples using the developed DPV methodology described in the previous section. The extraction of MePa and sample preparation is discussed in Section 2.5.

In order to compare the reliability of the electrochemical sensor, a UV-vis spectrophotometry comparative methodology was employed. Figure S3 shows the obtained calibration curve for the alternative methodology. The absorbance spectrum displayed a maximum absorbance peak at λ_{max} = 262 nm. The technique displayed a linear range from 1.0 to 60.0 µmol L^{-1} (R^2 = 0.996), with a LOD of 0.63 µmol L^{-1} and LOD of 2.10 µmol L^{-1}. Although the LOD and LOQ values for this technique were higher than the electrochemical one, comparison between the two techniques was possible. Figures S4 and S5 shows the DPV and UV-vis, respectively, detection of MePa in the real samples for hand sanitizer (A), mouthwash (B), deodorant (C), emollient for cuticles (D) and moisturizer cream (E) using the standard addition method (SAM), where the sample was spiked with known concentrations of the MePa standard.

Table 1. Comparison of the reported values for LOD of MePa.

Electrode	Linear Range (μmol L^{-1})	LOD (μmol L^{-1})	LOQ (μmol L^{-1})	Real Samples	Reference
Gold electrode	40–1000	1.71	5.70	Pharmaceutical products and urine	[55]
GCE/MWCNTs-LB	1.0–80	0.40	Not reported	Skin toner	[58]
Au/$(MNP/Ppy)_3$ electrode	0.0–131.40	0.0995	Not reported	Urine, breast milk and cosmetic	[29]
(Co-Ni-Pd)NPs-CNFs/GCE	0.003–0.3	0.0012	Not reported	Cosmetics, pharmaceuticals and urine samples	[59]
GCE/rGO/RuNPs	0.5–3.00	0.24	Not reported	Deodorant cream	[57]
AuNP-rGO-CS/GCE	0.03–1.30	0.0138	0.04173	Liquid soap, skin cleansing lotion, insect repellent and mouthwash	[27]
GC/RC-SbNPs	0.2–9.0	0.05	0.16	Hand sanitizer, mouthwash, deodorant, emollient for cuticles and moisturizer cream	This work

Au: gold electrode, AuNP: gold nanoparticles, CS: chitosan, MNP: magnetic nanoparticles, Ppy: polypirrol, GCE and GC: glassy carbon electrode, RuNPs: ruthenium nanoparticles, MWCNTs-LB: Langmuir–Blodgett (LB) film of multiwalled carbon nanotubes, (Co-Ni-Pd)NPs: cobalt, nickel and palladium nanoparticles, CNFs: carbon nanofibers.

The SAM method consisted in a quantitative analysis method, which is often used to overcome matrix effects in complexes samples. In that way, during analysis the sample (s) was spiked or enriched with known amounts of 1.0 µmol L^{-1} (a), 2.0 µmol L^{-1} (b) and 3.0 µmol L^{-1} (c). The method is performed by reading the experimental (I_{pa} or absorbance) intensity of the samples and then measuring the responses of the samples with amounts of known standard added. The data are plotted as I_{pa} or absorbance vs. the amount of the standard added. The least-squares line intersects the x-axis at the negative of the concentration of the unknown (Figures S4 and S5, respectively).

Table 2 shows the recovery of MePa using the SAM approach for the DPV and UV-vis techniques. The calculated error showed in Table 2 compared the concentration of MePa obtained between the two techniques (footnote). The hand sanitizer and mouthwash samples presented lower errors due to the extraction of MePa by liquid–liquid extraction (LLE) being more efficient in liquid samples than in those in semisolid (cream) consistency [60]. In addition, PCPs in creams and gel form might contain more fragrances, emulsifiers, ultraviolet filters, acrylates, preservatives, and antioxidants, which can interfere with UV-vis analysis due to such compounds having more chromophore groups (an unsaturated group that absorbs light) within their chemical structure [61–63]. In that way, a matrix effect would have less impact on the DPV electrochemical technique.

Table 2. Results for the determination of MePa by UV-vis and DPV techniques.

Samples	$DPV_{RECOVERED}$ (µmol L^{-1})	[2] Total MePa (µg/mL) DPV	UV-Vis	[1] Relative Error (%)
[3] Hand sanitizer	4.13 ± 0.10	50.30 ± 0.50	51.00 ± 0.50	−1.50
[3] Mouthwash	1.15 ± 0.05	49.22 ± 0.80	52.95 ± 0.92	−3.80
[4] Deodorant	0.38 ± 0.05	468.50 ± 2.60	513.51 ± 1.80	−8.80
[4] Emollient for cuticles	0.32 ± 0.03	394.50 ± 5.60	456.45 ± 2.20	−13.33
[4] Moisturizer cream	0.18 ± 0.04	221.40 ± 2.70	255.61 ± 1.50	−13.40

[1] Relative error: DPV vs. UV-vis ($C_{DPV} - C_{UV\text{-}vis}/C_{UV\text{-}vis}$) × 100%; [2] dilution correct between methods; [3] sample diluted 1:10 in ethanol; [4] sample diluted 1:10 in ethanol and then 1:100 in PBS.

Therefore, the developed DPV methodology using the GC/RC-SbNP sensor to detect MePa in PCPs was considered satisfactory. The error between the DPV and UV-vis comparative method was expected, especially in samples with a number of substances with chromophore groups being higher. In that way, the developed sensor could be a valuable tool to monitor MePa from an environmental perspective.

4. Conclusions

A novel electrochemical methodology for the detection of methylparaben in personal care products using a sensor based on renewable carbon and antimony nanoparticles was presented. The proposed material was successfully characterized by morphological and electrochemical techniques. The GC/RC-SbNP sensor was applied in the detection of MePa using DPV, presenting a sensitive, low-cost, and easy-to-prepare sensing platform. In addition, the proposed electrodes use a material obtained from bamboo waste, adding value to this waste.

Supplementary Materials: The following supporting information can be downloaded at https://www.mdpi.com/article/10.3390/chemosensors11020141/s1. Figure S1. (A) CV scans for GC (dashed line), GC/RC (black line), GC/RC-SbNPs (blue line), with a scan rate of 50 mVs^{-1}. (B) Nyquist diagrams for GC (▲), GC/RC (■) and GC/RC-SbNPs (●). Supporting electrolyte: 5 mmol L^{-1} of $[Fe(CN)_6]^{4-/3-}$ in 0.1 mol L^{-1} PBS and 0.1 mol L^{-1} KCl; Table S1: Fitted parameters of EIS experiments; Table S2: Fitted parameters of EIS experiments; Figure S2: Effect of RC-SbNP film concentration at I_{pa} of 10.0 µmol L^{-1} MePa. The DPV experiments were carried out in a 0.1 mol L^{-1} PBS pH 7.0; Figure S3: UV-vis spectra (220–350 nm) for different concentrations of MePa and the respective calibration curve showing the linear relationship of absorbance vs. [MePa]/µmol L^{-1}; Figure S4: Detection of MePa by proposed DPV method. The voltammograms for sample (s),

samples + 1.0 μmol L^{-1} (a), samples + 2.0 μmol L^{-1} (b) and samples + 3.0 μmol L^{-1} (c). For (A) hand sanitizer, (B) mouthwash, (C) deodorant, D) emollient for cuticles and E) moisturizer cream samples; Figure S5: UV-vis spectra and respective quantification of MePa concentrations for (A) hand sanitizer, (B) mouthwash, (C) deodorant, (D) emollient for cuticles and (E) moisturizer cream samples.

Author Contributions: Conceptualization—G.C.G. and I.C.; methodology—G.C.G. and M.K.L.d.S.; investigation—G.C.G., M.K.L.d.S. and F.C.B.; visualization—M.K.L.d.S. and I.C.; writing—original draft preparation, G.C.G.; writing—review and editing, M.K.L.d.S., F.C.B. and I.C.; supervision, I.C.; project administration, I.C.; funding acquisition, I.C. All authors have read and agreed to the published version of the manuscript.

Funding: This research received funding from FAPESP (grant 22/03762-8).

Institutional Review Board Statement: Not applicable.

Informed Consent Statement: Not applicable.

Data Availability Statement: Not applicable.

Acknowledgments: The authors also would like to acknowledge the LMA-IQ for the availability of the scanning electron microscope.

Conflicts of Interest: The authors declare no conflict of interest.

References

1. Madikizela, L.M.; Rimayi, C.; Khulu, S.; Chimuka, L.; Ncube, S. Pharmaceuticals and Personal Care Products. In *Emerging Freshwater Pollutants: Analysis, Fate and Regulations*; Elsevier: Amsterdam, The Netherlands, 2022; pp. 171–190, ISBN 9780128228500.
2. Osuoha, J.O.; Anyanwu, B.O.; Ejileugha, C. Pharmaceuticals and Personal Care Products as Emerging Contaminants: Need for Combined Treatment Strategy. *J. Hazard. Mater. Adv.* **2022**, *9*, 100206. [CrossRef]
3. AL Falahi, O.A.; Abdullah, S.R.S.; Hasan, H.A.; Othman, A.R.; Ewadh, H.M.; Kurniawan, S.B.; Imron, M.F. Occurrence of Pharmaceuticals and Personal Care Products in Domestic Wastewater, Available Treatment Technologies, and Potential Treatment Using Constructed Wetland: A Review. *Process Saf. Environ. Prot.* **2022**, *168*, 1067–1088. [CrossRef]
4. Farag Ambarak, M. Asian Journal of Green Chemistry Determination of Methylparaben in Some Cosmetics and Pharmaceutics Using Liquid-Liquid Extraction and Spectrophotometric Technique. *Asian J. Green Chem.* **2020**, *4*, 192–201. [CrossRef]
5. Li, J.; Han, Y.; Li, X.; Xiong, L.; Wei, L.; Cheng, X. Analysis of Methylparaben in Cosmetics Based on a Chemiluminescence $H_2O_2-NaIO_4-CNQDs$ System. *Luminescence* **2021**, *36*, 79–84. [CrossRef] [PubMed]
6. Heo, J.; Kwon, D.; Beirns, E.; Tan, G.Y.A.; Lee, P.H.; Kim, J. Superior Methylparaben Removal by Anaerobic Fluidized Bed Ceramic Membrane Bioreactor with PVDF Tubular Fluidized Biocarrier: Reactor Performance and Microbial Community. *J. Environ. Chem. Eng.* **2023**, *11*, 109153. [CrossRef]
7. Arvaniti, O.S.; Petala, A.; Zalaora, A.A.; Mantzavinos, D.; Frontistis, Z. Solar Light-Induced Photocatalytic Degradation of Methylparaben by g-C3N4 in Different Water Matrices. *J. Chem. Technol. Biotechnol.* **2020**, *95*, 2811–2821. [CrossRef]
8. Cetinić, K.A.; Grgić, I.; Previšić, A.; Rožman, M. The Curious Case of Methylparaben: Anthropogenic Contaminant or Natural Origin? *Chemosphere* **2022**, *294*, 133781. [CrossRef]
9. Hu, C.; Bai, Y.; Li, J.; Sun, B.; Chen, L. Endocrine Disruption and Reproductive Impairment of Methylparaben in Adult Zebrafish. *Food Chem. Toxicol.* **2023**, *171*, 113545. [CrossRef]
10. Nowak, K.; Jabłońska, E.; Garley, M.; Radziwon, P.; Ratajczak-Wrona, W. Methylparaben-Induced Regulation of Estrogenic Signaling in Human Neutrophils. *Mol. Cell. Endocrinol.* **2021**, *538*, 111470. [CrossRef] [PubMed]
11. Vieira, W.T.; De Farias, M.B.; Spaolonzi, M.P.; Da Silva, M.G.C.; Vieira, M.G.A. Endocrine-Disrupting Compounds: Occurrence, Detection Methods, Effects and Promising Treatment Pathways—A Critical Review. *J. Environ. Chem. Eng.* **2021**, *9*, 104558. [CrossRef]
12. Xue, J.; Wu, Q.; Sakthivel, S.; Pavithran, P.V.; Vasukutty, J.R.; Kannan, K. Urinary Levels of Endocrine-Disrupting Chemicals, Including Bisphenols, Bisphenol A Diglycidyl Ethers, Benzophenones, Parabens, and Triclosan in Obese and Non-Obese Indian Children. *Environ. Res.* **2015**, *137*, 120–128. [CrossRef] [PubMed]
13. De Carvalho Penha, L.C.; Coimbra Rola, R.; da Silva Junior, F.M.; de Martinez Gaspar Martins, C. Toxicity and Sublethal Effects of Methylparaben on Zebrafish (Danio Rerio) Larvae and Adults. *Environ. Sci. Pollut. Res.* **2021**, *28*, 45534–45544. [CrossRef] [PubMed]
14. Wei, F.; Mortimer, M.; Cheng, H.; Sang, N.; Guo, L.H. Parabens as Chemicals of Emerging Concern in the Environment and Humans: A Review. *Sci. Total Environ.* **2021**, *778*, 146150. [CrossRef] [PubMed]
15. Puerta, Y.T.; Guimarães, P.S.; Martins, S.E.; Martins, C.d.M.G. Toxicity of Methylparaben to Green Microalgae Species and Derivation of a Predicted No Effect Concentration (PNEC) in Freshwater Ecosystems. *Ecotoxicol. Environ. Saf.* **2020**, *188*, 109916. [CrossRef]

16. Nowak, K.; Ratajczak-Wrona, W.; Górska, M.; Jabłońska, E. Parabens and Their Effects on the Endocrine System. *Mol. Cell. Endocrinol.* **2018**, *474*, 238–251. [CrossRef]
17. Faradillawan Khalid, W.E.; Nasir Mat Arip, M.; Jasmani, L.; Heng Lee, Y. A New Sensor for Methyl Paraben Using an Electrode Made of a Cellulose Nanocrystal–Reduced Graphene Oxide Nanocomposite. *Sensors* **2019**, *19*, 2726. [CrossRef]
18. Marson, E.O.; Paniagua, C.E.S.; Gomes Júnior, O.; Gonçalves, B.R.; Silva, V.M.; Ricardo, I.A.; Maria, M.C.; Amorim, C.C.; Trovó, A.G. A Review toward Contaminants of Emerging Concern in Brazil: Occurrence, Impact and Their Degradation by Advanced Oxidation Process in Aquatic Matrices. *Sci. Total Environ.* **2022**, *836*, 155605. [CrossRef]
19. Khansari, N.; Adib, N.; Alikhani, A.; Babaee, T.; Khosrokhavar, R. Development and Validation of a New Method for Determination of Methylparaben in Iran Market Infant Formulae by HPLC. *J. Environ. Health Sci. Eng.* **2021**, *19*, 565–572. [CrossRef] [PubMed]
20. Sarfraz, S.; Hussain, S.; Javed, M.; Raza, A.; Iqbal, S.; Alrbyawi, H.; Aljazzar, S.O.; Elkaeed, E.B.; Somaily, H.H.; Pashameah, R.A.; et al. Simultaneous HPLC Determination of Clindamycin Phosphate, Tretinoin, and Preservatives in Gel Dosage Form Using a Novel Stability-Indicating Method. *Inorganics* **2022**, *10*, 168. [CrossRef]
21. De Almeida Brehm Goulart, F.; Reichert, G.; Felippe, T.C.; Mizukawa, A.; Antonelli, J.; Fernandes, C.S.; de Azevedo, J.C.R. Daily Variation of Lipid Regulators and Personal Care Products in a River Impacted by Domestic Effluents in Southern Brazil. *Water* **2021**, *13*, 1393. [CrossRef]
22. Dos Santos, M.M.; Brehm, F.d.A.; Filippe, T.C.; Knapik, H.G.; de Azevedo, J.C.R. Ocorrência e Avaliação de Risco de Parabenos e Triclosan Em Águas Superficiais Na Região Sul Do Brasil: Um Problema de Poluentes Emergentes Em Um País Emergente. *Rev. Bras. Recur. Hidr.* **2016**, *21*, 603–617. [CrossRef]
23. Dualde, P.; Pardo, O.; FFernández, S.; Pastor, A.; Yusà, V. Determination of Four Parabens and Bisphenols A, F and S in Human Breast Milk Using QuEChERS and Liquid Chromatography Coupled to Mass Spectrometry. *J. Chromatogr. B Anal. Technol. Biomed. Life Sci.* **2019**, *1114–1115*, 154–166. [CrossRef] [PubMed]
24. Kaya, S.I.; Cetinkaya, A.; Bakirhan, N.K.; Ozkan, S.A. Trends in Sensitive Electrochemical Sensors for Endocrine Disruptive Compounds. *Trends Environ. Anal. Chem.* **2020**, *28*, e00106. [CrossRef]
25. Silwana, B.; van der Horst, C.; Iwuoha, E.; Somerset, V. Reduced Graphene Oxide Impregnated Antimony Nanoparticle Sensor for Electroanalysis of Platinum Group Metals. *Electroanalysis* **2016**, *28*, 1597–1607. [CrossRef]
26. Oliveira, T.M.B.F.; Ribeiro, F.W.P.; Sousa, C.P.; Salazar-Banda, G.R.; de Lima-Neto, P.; Correia, A.N.; Morais, S. Current Overview and Perspectives on Carbon-Based (Bio)Sensors for Carbamate Pesticides Electroanalysis. *TrAC Trends Anal. Chem.* **2020**, *124*, 115779. [CrossRef]
27. Piovesan, J.V.; Santana, E.R.; Spinelli, A. Reduced Graphene Oxide/Gold Nanoparticles Nanocomposite-Modified Glassy Carbon Electrode for Determination of Endocrine Disruptor Methylparaben. *J. Electroanal. Chem.* **2018**, *813*, 163–170. [CrossRef]
28. Mielech-Łukasiewicz, K.; Bliźniukiewicz, A. Electrochemical Oxidation and Determination of Methylparaben at Overoxidized Polypyrrole Film Modified a Boron-Doped Diamond Electrode. *J. Iran. Chem. Soc.* **2018**, *15*, 2703–2711. [CrossRef]
29. De Lima, L.F.; Daikuzono, C.M.; Miyazaki, C.M.; Pereira, E.A.; Ferreira, M. Layer-by-Layer Nanostructured Films of Magnetite Nanoparticles and Polypyrrole towards Synergistic Effect on Methylparaben Electrochemical Detection. *Appl. Surf. Sci.* **2020**, *505*, 144278. [CrossRef]
30. Santana, E.R.; Spinelli, A. Electrode Modified with Graphene Quantum Dots Supported in Chitosan for Electrochemical Methods and Non-Linear Deconvolution of Spectra for Spectrometric Methods: Approaches for Simultaneous Determination of Triclosan and Methylparaben. *Microchim. Acta* **2020**, *187*, 250. [CrossRef]
31. Baig, N.; Sajid, M.; Saleh, T.A. Recent Trends in Nanomaterial-Modified Electrodes for Electroanalytical Applications. *TrAC Trends Anal. Chem.* **2019**, *111*, 47–61. [CrossRef]
32. Spanu, D.; Binda, G.; Dossi, C.; Monticelli, D. Biochar as an Alternative Sustainable Platform for Sensing Applications: A Review. *Microchem. J.* **2020**, *159*, 105506. [CrossRef]
33. Nan, N.; DeVallance, D.B.; Xie, X.; Wang, J. The Effect of Bio-Carbon Addition on the Electrical, Mechanical, and Thermal Properties of Polyvinyl Alcohol/Biochar Composites. *J. Compos. Mater.* **2016**, *50*, 1161–1168. [CrossRef]
34. Arnold, S.; Rodriguez-Uribe, A.; Misra, M.; Mohanty, A.K. Slow Pyrolysis of Bio-Oil and Studies on Chemical and Physical Properties of the Resulting New Bio-Carbon. *J. Clean. Prod.* **2016**, *172*, 2748–2758. [CrossRef]
35. Agustini, D.; Mangrich, A.S.; Bergamini, M.F.; Marcolino-Junior, L.H. Sensitive Voltammetric Determination of Lead Released from Ceramic Dishes by Using of Bismuth Nanostructures Anchored on Biochar. *Talanta* **2015**, *142*, 221–227. [CrossRef] [PubMed]
36. Gevaerd, A.; De Oliveira, P.R.; Mangrich, A.S.; Bergamini, M.F.; Marcolino-Junior, L.H. Evaluation of Antimony Microparticles Supported on Biochar for Application in the Voltammetric Determination of Paraquat. *Mater. Sci. Eng. C* **2016**, *62*, 123–129. [CrossRef]
37. De Oliveira, P.R.; Kalinke, C.; Gogola, J.L.; Mangrich, A.S.; Junior, L.H.M.; Bergamini, M.F. The Use of Activated Biochar for Development of a Sensitive Electrochemical Sensor for Determination of Methyl Parathion. *J. Electroanal. Chem.* **2017**, *799*, 602–608. [CrossRef]
38. Martins, G.; Gogola, J.L.; Caetano, F.R.; Kalinke, C.; Jorge, T.R.; Santos, C.N.D.; Bergamini, M.F.; Marcolino-Junior, L.H. Quick Electrochemical Immunoassay for Hantavirus Detection Based on Biochar Platform. *Talanta* **2019**, *204*, 163–171. [CrossRef]

39. Valenga, M.G.P.; Martins, G.; Martins, T.A.C.; Didek, L.K.; Gevaerd, A.; Marcolino-Junior, L.H.; Bergamini, M.F. Biochar: An Environmentally Friendly Platform for Construction of a SARS-CoV-2 Electrochemical Immunosensor. *Sci. Total Environ.* **2023**, *858*, 159797. [CrossRef]
40. He, R.; Yuan, X.; Huang, Z.; Wang, H.; Jiang, L.; Huang, J.; Tan, M.; Li, H. Activated Biochar with Iron-Loading and Its Application in Removing Cr (VI) from Aqueous Solution. *Colloids Surfaces A Physicochem. Eng. Asp.* **2019**, *579*, 123642. [CrossRef]
41. Chacón, F.J.; Sánchez-Monedero, M.A.; Lezama, L.; Cayuela, M.L. Enhancing Biochar Redox Properties through Feedstock Selection, Metal Preloading and Post-Pyrolysis Treatments. *Chem. Eng. J.* **2020**, *395*, 125100. [CrossRef]
42. Ji, L.; Spanu, D.; Denisov, N.; Recchia, S.; Schmuki, P.; Altomare, M. A Dewetted-Dealloyed Nanoporous Pt Co-Catalyst Formed on TiO2 Nanotube Arrays Leads to Strongly Enhanced Photocatalytic H2 Production. *Chem. Asian J.* **2020**, *15*, 301–309. [CrossRef] [PubMed]
43. Moraes, F.C.; Cesarino, I.; Cesarino, V.; Mascaro, L.H.; MacHado, S.A.S. Carbon Nanotubes Modified with Antimony Nanoparticles: A Novel Material for Electrochemical Sensing. *Electrochim. Acta* **2012**, *85*, 560–565. [CrossRef]
44. Silva, M.K.L.L.; Cesarino, I. Electrochemical Sensor Based on Sb Nanoparticles/Reduced Graphene Oxide for Heavy Metal Determination. *Int. J. Environ. Anal. Chem.* **2020**, *102*, 3109–3123. [CrossRef]
45. Serrano, N.; Díaz-Cruz, J.M.; Ariño, C.; Esteban, M. Antimony- Based Electrodes for Analytical Determinations. *TrAC Trends Anal. Chem.* **2016**, *77*, 203–213. [CrossRef]
46. Nunes, E.W.; Silva, M.K.L.; Cesarino, I. Evaluation of a Reduced Graphene Oxide-Sb Nanoparticles Electrochemical Sensor for the Detection of Cadmium and Lead in Chamomile Tea. *Chemosensors* **2020**, *8*, 53. [CrossRef]
47. Hasegawa, K.; Minakata, K.; Suzuki, M.; Suzuki, O. The Standard Addition Method and Its Validation in Forensic Toxicology. *Forensic Toxicol.* **2021**, *39*, 311–333. [CrossRef]
48. Cesarino, I.; Cincotto, F.H.; Machado, S.A.S. A Synergistic Combination of Reduced Graphene Oxide and Antimony Nanoparticles for Estriol Hormone Detection. *Sens. Actuators B Chem.* **2015**, *210*, 453–459. [CrossRef]
49. Sebez, B.; Ogorevc, B.; Hocevar, S.B.; Veber, M. Functioning of Antimony Film Electrode in Acid Media under Cyclic and Anodic Stripping Voltammetry Conditions. *Anal. Chim. Acta* **2013**, *785*, 43–49. [CrossRef]
50. Gil, E.d.S.; Andrade, C.H.; Barbosa, N.L.; Braga, R.C.; Serrano, S.H.P.P. Cyclic Voltammetry and Computational Chemistry Studies on the Evaluation of the Redox Behavior of Parabens and Other Analogues. *J. Braz. Chem. Soc.* **2012**, *23*, 565–572. [CrossRef]
51. Qian, K.; Kumar, A.; Zhang, H.; Bellmer, D.; Huhnke, R. Recent Advances in Utilization of Biochar. *Renew. Sustain. Energy Rev.* **2015**, *42*, 1055–1064. [CrossRef]
52. Cesarino, I.; Cesarino, V.; Lanza, M.R.V. Carbon Nanotubes Modified with Antimony Nanoparticles in a Paraffin Composite Electrode: Simultaneous Determination of Sulfamethoxazole and Trimethoprim. *Sens. Actuators B Chem.* **2013**, *188*, 1293–1299. [CrossRef]
53. Da Silva, M.K.L.; Plana Simões, R.; Cesarino, I. Evaluation of Reduced Graphene Oxide Modified with Antimony and Copper Nanoparticles for Levofloxacin Oxidation. *Electroanalysis* **2018**, *30*, 2066–2076. [CrossRef]
54. Da Silveira, J.P.; Piovesan, J.V.; Spinelli, A. Carbon Paste Electrode Modified with Ferrimagnetic Nanoparticles for Voltammetric Detection of the Hormone Estriol. *Microchem. J.* **2017**, *133*, 22–30. [CrossRef]
55. Naik, K.M.; Nandibewoor, S.T. Electroanalytical Method for the Determination of Methylparaben. *Sens. Actuators A Phys.* **2014**, *212*, 127–132. [CrossRef]
56. Błedzka, D.; Gromadzińska, J.; Wasowicz, W. Parabens. From Environmental Studies to Human Health. *Environ. Int.* **2014**, *67*, 27–42. [CrossRef] [PubMed]
57. Mendonça, C.D.; Prado, T.M.; Cincotto, F.H.; Verbinnen, R.T.; Machado, S.A.S. Methylparaben Quantification via Electrochemical Sensor Based on Reduced Graphene Oxide Decorated with Ruthenium Nanoparticles. *Sens. Actuators B Chem.* **2017**, *251*, 739–745. [CrossRef]
58. Wang, L.; Li, Y.; Li, G.; Ye, B. A New Strategy for Enhancing Electrochemical Sensing from MWCNTs Modified Electrode with Langmuir-Blodgett Film and Used in Determination of Methylparaben. *Sens. Actuators B Chem.* **2015**, *211*, 332–338. [CrossRef]
59. Baytak, A.K.; Duzmen, S.; Teker, T.; Aslanoglu, M. Voltammetric Determination of Methylparaben and Its DNA Interaction Using a Novel Platform Based on Carbon Nanofibers and Cobalt-Nickel-Palladium Nanoparticles. *Sens. Actuators B Chem.* **2017**, *239*, 330–337. [CrossRef]
60. Chormey, D.S.; Zaman, B.T.; Kasa, N.A.; Bakırdere, S. Liquid Phase Microextraction Strategies and Their Application in the Determination of Endocrine Disruptive Compounds in Food Samples. *TrAC Trends Anal. Chem.* **2020**, *128*, 115917. [CrossRef]
61. Chakraborty, J.N. Colouring Materials. *Fundam. Pract. Colouration Text.* **2010**, 11–19. [CrossRef]
62. Calvo, F.; Gómez, J.M.; Ricardez-Sandoval, L.; Alvarez, O. Integrated Design of Emulsified Cosmetic Products: A Review. *Chem. Eng. Res. Des.* **2020**, *161*, 279–303. [CrossRef]
63. Duis, K.; Junker, T.; Coors, A. Review of the Environmental Fate and Effects of Two UV Filter Substances Used in Cosmetic Products. *Sci. Total Environ.* **2022**, *808*, 151931. [CrossRef] [PubMed]

Disclaimer/Publisher's Note: The statements, opinions and data contained in all publications are solely those of the individual author(s) and contributor(s) and not of MDPI and/or the editor(s). MDPI and/or the editor(s) disclaim responsibility for any injury to people or property resulting from any ideas, methods, instructions or products referred to in the content.